Organic LETTERS

Letter

pubs.acs.org/OrgLett

Dual Emission and Mechanofluorochromism of a V-Shaped π-System Composed of Disulfonyl-Substituted Dibenzocyclooctatetraenes

Takanori Nishida,[†] Shinya Ohta,[†] Feng Xu,[†] Kenta Shinohara,[†] Takahiro Kamada,[‡] Haruo Akashi,[‡] Makoto Takezaki,[†] Kan Wakamatsu,[§] and Akihiro Orita*[,†]

[†]Department of Applied Chemistry and Biotechnology, Okayama University of Science, 1-1 Ridai-cho, Kita-ku, Okayama 700-0005, Japan

[‡]Research Institute of Natural Sciences, Okayama University of Science, 1-1 Ridai-cho, Kita-ku, Okayama 700-0005 Japan

[§]Department of Chemistry, Okayama University of Science, 1-1 Ridai-cho, Kita-ku, Okayama 700-0005, Japan

Supporting Information

ABSTRACT: A series of dibenzocyclooctatetraenes **6** bearing phenylethynyl and phenylsulfonyl groups were synthesized from bromo-substituted formylbenzyl sulfone **4** via cyclic dimerization of **4** and Sonogashira coupling of the resulting dibromocyclooctatetraene **3** with terminal acetylenes. The diamino derivative **6b** exhibited dual emission with emission maxima at 436 and 547 nm. Furthermore, in the fluorescence of **6b**, solvatofluorochromism was observed in response to solvent polarity, whereas in the solid states, mechanofluorochromism was observed.

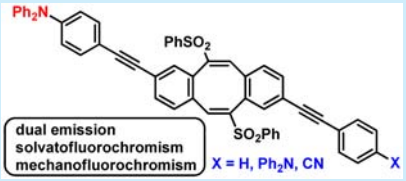

Expanded π-systems have attracted significant attention from researchers because they can be used as materials in organic light-emitting diodes (OLEDs)[1] and organic field-effect transistors (OFETs)[2] and as dyes in organic solar cells (OSCs).[3] In general, these materials possess an expanded monoplanar array of aromatic moieties and exhibit efficient π-conjugation. Recently, a V-shaped anthracenimide π-system was synthesized, and its novel environment-dependent optical properties were reported.[4] Consequently, in order to access these interesting V-shaped π-systems, we previously developed a synthetic method for the synthesis of "magazine-rack" molecules, which are composed of diarylethynes connected by *cis*-ethenylenes (Scheme 1).[5] Although this protocol is useful

Scheme 1. Synthesis of Magazine-Rack Molecules

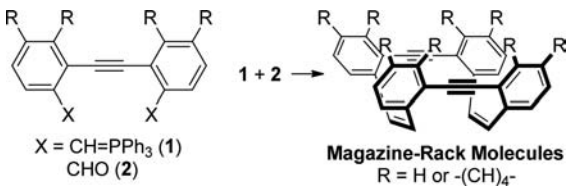

in the synthesis of benzo and naphtho derivatives, it suffers from time-consuming and laborious operation at larger scales because the precursors of the Wittig olefinations (**1** and **2**) show poor solubility in common organic solvents. Therefore, in order to realize a systematic synthesis of V-shaped π-systems and investigate their optical and physical properties, we used bromo-substituted dibenzocyclooctatetraene **3** as a key precursor; **3** may be prepared easily via the cyclic dimerization of formyl sulfone **4** (Scheme 2). We envisioned that Sonogashira coupling of **3** with terminal ethynes **5** would provide a series of acetylenic V-shaped π-systems such as **6a**–**d**.

Scheme 2. Synthetic Plan for 6a–c[a]

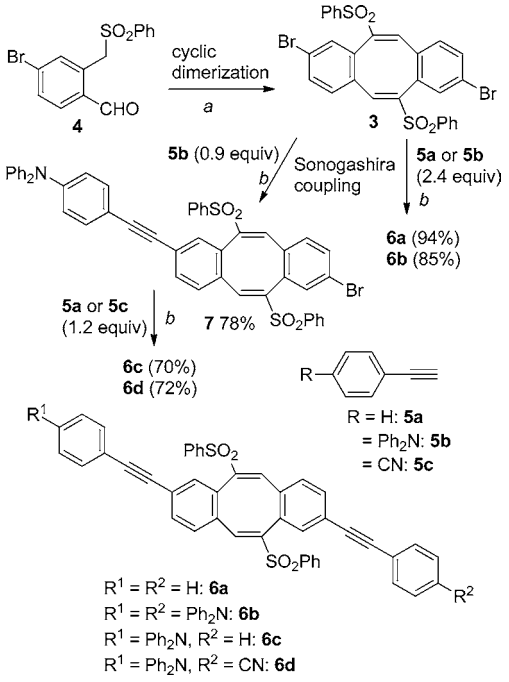

[a]Reagents and conditions: (*a*) $ClP(O)(OEt)_2$ (1.2 equiv), LiHMDS (1.2 equiv), THF, −78 °C, 0.5 h to rt, 18 h. (*b*) $Pd(PPh_3)_4$ (10 mol %), CuI (10 mol %), toluene, i-Pr_2NH, 80 °C, 18 h.

Because the V-shaped compounds **6a**–**d** have two electron-withdrawing phenylsulfonyl groups on the dibenzocyclooctate-

Received: June 20, 2016
Published: August 5, 2016

DOI: 10.1021/acs.orglett.6b01786
Org. Lett. 2016, 18, 3988–3991

traene moieties, it was expected that amino-substituted derivatives **6b–d** would undergo intramolecular charge transfer upon photoexcitation. We also expected that the bulkiness of the phenylsulfonyl groups would prevent flipping of the dibenzocyclooctatetraene moiety, leading to efficient fluorescence.[4c] Thus, we herein report the syntheses of disulfonyl-substituted dibenzocyclooctatetraenes **6a–d** and their optical properties, including UV–vis absorption and photoluminescence spectra.

In a previous study, we reported the efficient syntheses of several disulfonyl-substituted dibenzocyclooctatetraenes such as **3** and **6**, which are precursors of diarenocyclooctadiynes (i.e., Sondheimer–Wong diynes).[6] This synthetic method was applied to the syntheses of **6a–d** (Scheme 2). Treatment of **4** with diethyl chlorophosphate and lithium hexamethyldisilazide (LiHMDS) gave **3** in 51% yield. Sonogashira couplings of **3** with 2 equiv of phenylethynes **5a** and **5b** afforded the desired cyclooctatetraenes **6a** and **6b** in 94% and 85% yield, respectively. Unsymmetrically substituted derivatives **6c** and **6d** were synthesized using **7** in stepwise Sonogashira couplings. Sonogashira coupling of **3** with **5b** afforded amino bromide **7** in 78% yield, and successive couplings of **7** with **5a** and **5c** afforded the monoamino derivative **6c** and the amino/cyano derivative **6d** in 70% and 66% yield, respectively.

Recrystallization of **6a** from acetonitrile provided a single crystal suitable for single-crystal X-ray diffraction measurements, and the diffraction data confirmed the V-shaped structure of the bis(phenylethynyl)dibenzocyclooctatetraene moiety in **6a** (Figure S1).[7] In solid-state **6a**, the dihedral angle between the ethynylene-connected benzene rings is 31.8°; this confirms the efficient expansion of the π-system in the diphenylethyne moieties.

The optical properties of the V-shaped molecules **6a–d**, including their UV–vis absorption and photoluminescence spectra, were recorded in CH_2Cl_2 (Figure 1), and these data are summarized in Table 1.

In the UV–vis absorption spectra, **6a** shows an absorption band at 307 nm (ε = 59 200 L mol^{-1} cm^{-1}), whereas amino-substituted derivatives **6b–d** show an absorption band at 375 nm. The molar extinction coefficients (ε) at 375 nm are tunable by the substitution pattern and are 73 700, 43 500, and 35 700 L mol^{-1} cm^{-1} for the diamino derivative **6b**, monoamino derivative **6c**, and amino/cyano derivative **6d**, respectively. Time-dependent density functional theory (TD-DFT) calculations (B3LYP/6-31G(d)) indicated that the absorption bands of **6a–d** at the longest wavelengths can be assigned mainly to the highest occupied molecular orbital (HOMO)–lowest unoccupied molecular orbital (LUMO) transition. When **6a–d** in CH_2Cl_2 (1.0×10^{-6} M) are irradiated with UV light, photoluminescence is observed in low to moderate quantum yields (Figure 1b). Although phenylethynyl derivative **6a** exhibits a weak emission at 430 nm, amino-substituted derivatives **6b–d** exhibit stronger emission at longer wavelengths. In the photoluminescence measurements, diamino derivative **6b** and monoamino derivative **6c** exhibit moderate quantum yields (0.49 and 0.41, respectively), but the amino/cyano derivative **6d** exhibits a low quantum yield (0.08). It is noteworthy that the amino derivatives **6b–d** exhibit two separate emission maxima (dual emission), e.g., 436 and 547 nm for **6b**.[8,9] The emissions observed at the shorter and longer wavelengths are herein termed as emission A (denoted by the red dot in Figure 1b) and emission B (the blue dot), respectively.[10−12]

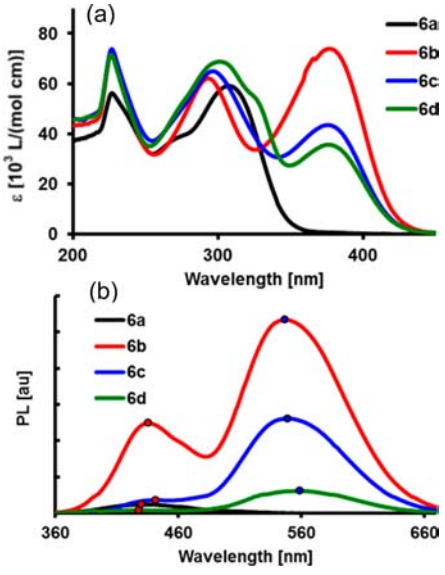

Figure 1. (a) UV–vis absorption and (b) photoluminescence spectra of **6a–d** (in CH_2Cl_2, (a) 1.0×10^{-4} M, (b) 1.0×10^{-6} M).

Table 1. Summary of UV–Vis Absorption[a] and Photoluminescence Spectra[b] of 6a–d

compound	λ_{max}[c] (nm) (ε)[d]/simulated λ_{max}[e] (nm) (f)[f]	E_{max} (nm)/Φ_F[g]
6a	307 (59.2)/360.3 (0.121)	430/0.03
6b	375 (73.7)/442.0 (0.789)	436, 547/0.49
6c	375 (43.5)/443.4 (0.389)	442, 549/0.41
6d	375 (35.7)/489.4 (0.041)	428, 559/0.08

[a]In CH_2Cl_2 (1.0×10^{-4} M). [b]In CH_2Cl_2 (1.0×10^{-6} M). [c]Absorption band observed at the longest wavelength. [d]In units of 10^3 L mol^{-1} cm^{-1}. [e]Calculated at the B3LYP/6-31G(d) level. [f]Oscillator strength. [g]Absolute fluorescence quantum yield.

To investigate the dual emission observed in **6b–d**, the photoluminescence of **6b** was recorded in a series of solvents, including cyclohexane (c-hex), benzene, $CHCl_3$, tetrahydrofuran (THF), CH_2Cl_2, and acetonitrile. Pronounced solvatofluorochromism was observed, as the emission color of **6b** changed from blue to orange in response to the solvent polarity (Figure 2 and Table 2). In each solvent, dual emission was observed: emission A underwent a red shift of 66 nm (c-hex → MeCN), and emission B exhibited a larger bathochromic shift of 105 nm (c-hex → CH_2Cl_2).[13] When these two emissions for **6b** were recorded in CH_2Cl_2 by changing the wavelength of the excitation light (300–390 nm), two independent excitation maxima were observed: emission A was maximal upon excitation at 350 nm, whereas emission B was maximal at 390 nm (Figure S2).[14] Lippert–Mataga plots are a powerful tool for quantitative evaluation of the change in dipole moment ($|\mu_e - \mu_g|$) upon photoexcitation.[15] Using a Lippert–Mataga plot, we found that emission B from **6b** is more dependent on the solvent dipole moment than emission A ($|\mu_e - \mu_g|$ = 28.0 and 33.9 D for emissions A and B, respectively).[16] These phenomena indicate that emissions A and B are ascribable to relaxation from different excited states.

To investigate the mechanism of the dual emission observed in this study, DFT calculations were performed for **6b** at the B3LYP/6-31G(d) level. The HOMO and LUMO of **6b** are representatively shown in Figure 3. The HOMO and LUMO

DOI: 10.1021/acs.orglett.6b01786
Org. Lett. 2016, 18, 3988–3991

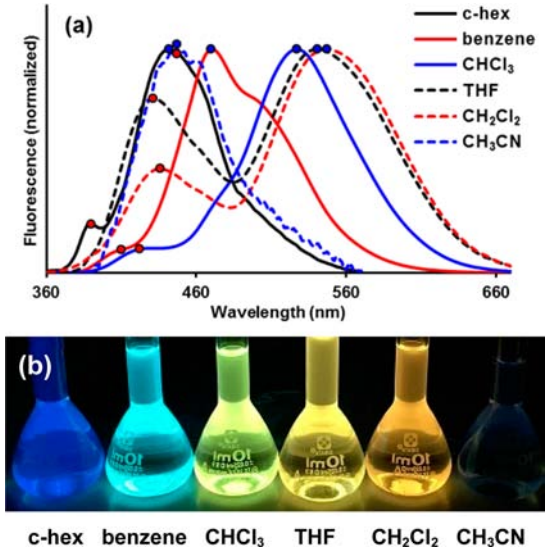

Figure 2. (a) Photoluminescence profiles and (b) pictures of **6b** in a series of solvents (1.0×10^{-6} M).

Table 2. Summary of Photoluminescence of 6b in a Series of Solvents

	E_{max}[a] (nm)		
solvent	emission A	emission B	Φ_F[b]
c-hex[c]	390	442	0.58
C_6H_6	410	470	0.82
$CHCl_3$	422	527	0.84
THF	431	541	0.46
CH_2Cl_2	436	547	0.49
CH_3CN[c]	456	nd	0.04

[a]In solution (1.0×10^{-6} M). [b]Absolute fluorescence quantum yield. [c]Concentration not determined because of the poor solubility of **6b**.

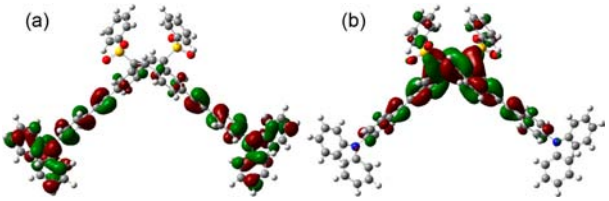

Figure 3. (a) HOMO and (b) LUMO of **6b**.

are located mainly in the outer and central parts of **6b**, respectively. In the HOMO, lone pairs on the amino nitrogen atoms play a pivotal role in π-system expansion, and in the LUMO, the antibonding orbitals of the ethenylenes in the dibenzocyclooctatetraene and the ethynylenes in the diphenylethyne moieties serve to promote the expansion of the π-system.

The simulated absorption spectrum, comprising a linear combination of oscillator strengths obtained via TD-DFT calculations, shows good agreement with the UV−vis absorption and excitation profiles (Figure S3 and Table S1). A comparison of these profiles suggests that emissions A and B should be assigned to radiative transitions from different singlet states, to which processes the electronic transitions (HOMO or HOMO−1)/LUMO+1 and HOMO/LUMO, respectively, contribute significantly (Figure S4).

When crystals of **6a−d** obtained from recrystallization in acetonitrile were irradiated with UV light, they also exhibited fluorescence. The emission maxima (E_{max}) of these crystals were recorded in the range of 439−502 nm (Figure S5 and Table 3). Although the amino/cyano derivative **6d** showed the highest fluorescence quantum yield (Φ_F = 0.43), the quantum yield decreased significantly (from 0.43 to 0.15) for a film fabricated via evaporation of an AcOEt solution of **6d**.[17,18] It is intriguing that amino derivatives **6b−d** exhibit mechanofluorochromism and that the thin films of **6b−d** undergo a bathochromic shift in emission upon grinding with a mortar and pestle (ΔE_{max} = 55 nm for **6b** and **6c** and 73 nm for **6d**).[18,19] For instance, **6d** exhibits sky-blue and yellow emission in a fabricated film and ground powder, respectively, upon irradiation with UV light (Figure 4), and this mechanofluorochromism can be switched by refabricating (i.e., dissolving the ground powder in AcOEt followed by evaporation) and grinding the film (Figure 4 inset).

Table 3. Summary of Photoluminescence of 6a−d in the Solid State

	E_{max} (nm) (Φ_F)[a]		
compound	crystals[b]	film[c]	powder[d]
6a	439 (0.12)	435 (0.05)	437 (0.08)
6b	468 (0.36)	463 (0.58)	518 (0.51)
6c	465 (0.15)	463 (0.21)	518 (0.17)
6d	475, 502 (0.43)	449 (0.15)	522 (0.26)

[a]Absolute fluorescence quantum yield. [b]Recrystallized from acetonitrile. [c]Film evaporated from ethyl acetate. [d]Ground with a mortar and pestle.

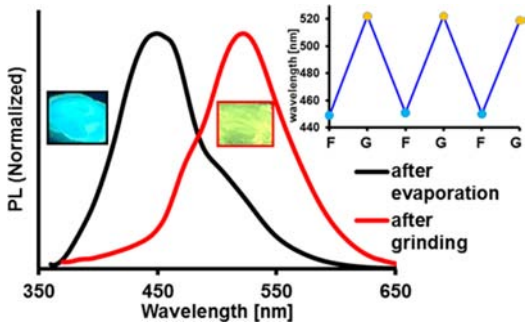

Figure 4. Emission profiles of **6d** in the fabricated film and ground powder states. The inset shows E_{max} in mechanofluorochromism (F, film; G, ground powder).

In summary, we synthesized a series of disulfonyl-substituted dibenzocyclooctatetraenes with a rigid V-shaped π-system. The V-shaped structure was confirmed via single-crystal X-ray diffraction analysis. These acetylenic dibenzocyclooctatetraenes emitted fluorescence under UV light, and in the amino-substituted derivatives, dual emission was observed. In the solid state, the above-mentioned compounds exhibited mechanofluorochromism, and their emission wavelengths and fluorescence quantum yields changed according to the solidification method and/or physical stimulus. Further investigations of the optical properties of the V-shaped π-systems and their application to organic materials are underway.

DOI: 10.1021/acs.orglett.6b01786
Org. Lett. 2016, 18, 3988−3991

■ ASSOCIATED CONTENT

Supporting Information

The Supporting Information is available free of charge on the ACS Publications website at DOI: 10.1021/acs.orglett.6b01786.

Full experimental and characterization data for all compounds and X-ray crystallographic data for **6a** (PDF)

■ AUTHOR INFORMATION

Corresponding Author

*orita@dac.ous.ac.jp

Notes

The authors declare no competing financial interest.

■ ACKNOWLEDGMENTS

This work was supported by JSPS KAKENHI Grants JP16H01164 in Middle Molecular Strategy and JP15K05440, the Okayama Prefecture Industrial Promotion Foundation and Grant for Promotion of OUS Research Projects.

■ REFERENCES

(1) (a) Müllen, K.; Scherf, U. *Organic Light Emitting Devices: Synthesis, Properties and Applications*; Wiley-VCH: Weinheim, Germany, 2006. (b) Yersin, H. *Highly Efficient OLEDs with Phosphorescent Materials*; Wiley-VCH: Weinheim, Germany, 2008. (c) Tsujimura, T. *OLED Display Fundamentals and Applications*; Wiley: Hoboken, NJ, 2012. (d) Yang, X.; Zhou, G.; Wong, W.-Y. *Chem. Soc. Rev.* **2015**, *44*, 8484.

(2) (a) Wöll, C. *Organic Electronics: Structural and Electronic Properties of OFETs*; Wiley-VCH: Weinheim, Germany, 2009. (b) Bunz, U. H. F. *Acc. Chem. Res.* **2015**, *48*, 1676. (c) Ward, J. W.; Lamport, Z. A.; Jurchescu, O. D. *ChemPhysChem* **2015**, *16*, 1118. (d) Zhang, C.; Chen, P.; Hu, W. *Chem. Soc. Rev.* **2015**, *44*, 2087. (e) Zhang, L.; Cao, Y.; Colella, N. S.; Liang, Y.; Bredas, J.-L.; Houk, K. N.; Briseno, A. L. *Acc. Chem. Res.* **2015**, *48*, 500. (f) Jiang, W.; Li, Y.; Wang, Z. *Acc. Chem. Res.* **2014**, *47*, 3135.

(3) (a) Ashford, D. L.; Gish, M. K.; Vannucci, A. K.; Brennaman, M. K.; Templeton, J. L.; Papanikolas, J. M.; Meyer, T. J. *Chem. Rev.* **2015**, *115*, 13006. (b) Chaurasia, S.; Liang, C.-J.; Yen, Y.-S.; Lin, J. T. *J. Mater. Chem. C* **2015**, *3*, 9765. (c) Collavini, S.; Völker, S. F.; Delgado, J. L. *Angew. Chem., Int. Ed.* **2015**, *54*, 9757. (d) Liu, Z.; Lau, S. P.; Yan, F. *Chem. Soc. Rev.* **2015**, *44*, 5638. (e) Chen, G.; Sasabe, H.; Igarashi, T.; Hong, Z.; Kido, J. *J. Mater. Chem. A* **2015**, *3*, 14517. (f) Jakubikova, E.; Bowman, D. N. *Acc. Chem. Res.* **2015**, *48*, 1441. (g) Calogero, G.; Bartolotta, A.; Di Marco, G.; Di Carlo, A.; Bonaccorso, F. *Chem. Soc. Rev.* **2015**, *44*, 3244.

(4) (a) Yuan, C.; Saito, S.; Camacho, C.; Irle, S.; Hisaki, I.; Yamaguchi, S. *J. Am. Chem. Soc.* **2013**, *135*, 8842. (b) Yuan, C.; Saito, S.; Camacho, C.; Kowalczyk, T.; Irle, S.; Yamaguchi, S. *Chem. - Eur. J.* **2014**, *20*, 2193. (c) Nishiuchi, T.; Tanaka, K.; Kuwatani, Y.; Sung, J.; Nishinaga, T.; Kim, D.; Iyoda, M. *Chem. - Eur. J.* **2013**, *19*, 4110.

(5) Orita, A.; Jiang, L.; Tsuruta, M.; Otera, J. *Chem. Lett.* **2002**, *31*, 136.

(6) (a) Xu, F.; Peng, L.; Shinohara, K.; Morita, T.; Yoshida, S.; Hosoya, T.; Orita, A.; Otera, J. *J. Org. Chem.* **2014**, *79*, 11592. (b) Orita, A.; Hasegawa, D.; Nakano, T.; Otera, J. *Chem. - Eur. J.* **2002**, *8*, 2000.

(7) CCDC 1469984 contains the supplementary crystallographic data for **6a**.

(8) Although several sulfones exhibiting dual emission have been reported, these instances are ascribable to (a) individual emissions from D−A−D′-type sulfones bearing a couple of different donors or (b) simultaneous fluorescence and phosphorescence from iodine-substituted crystalline sulfones. See: (a) Xie, Z.; Chen, C.; Xu, S.; Li, J.; Zhang, Y.; Liu, S.; Xu, J.; Chi, Z. *Angew. Chem., Int. Ed.* **2015**, *54*, 7181. (b) Mao, Z.; Yang, Z.; Mu, Y.; Zhang, Y.; Wang, Y.-F.; Chi, Z.; Lo, C.-C.; Liu, S.; Lien, A.; Xu, J. *Angew. Chem., Int. Ed.* **2015**, *54*, 6270.

(9) DFT calculations demonstrated that the $PhSO_2$-substituted dibenzocyclooctatetraene moiety changed to a shallow V-shaped structure in the excited state of a model compound of **6b**, whereas it was reported that a dianthrocyclooctatetraene derivative underwent planarization in the S_1 state. See ref 4 and the Supporting Information for details.

(10) When the photoluminescence of **6b** was recorded under argon or air, the relative intensity of emissions A and B was constant, supporting that both emissions A and B would be fluorescence not phosphorescence. See Figure S6 for details.

(11) Although it has been reported that upon photoexcitation a dianthracenocyclooctatetraene scaffold in solution would adopt a planar conformation (see ref 4a), DFT calculations indicated that the steric hindrance of sulfonyl groups would prevent planarization of **6a**−**d**. See the Supporting Information for details.

(12) See Figures S7−S9 for emission profiles of **6a**, **6c**, and **6d**, respectively, in a series of solvents.

(13) In MeCN, emission B was not observed, and this quenching could be explained in terms of nonfluorescent thermal relaxation from the excited state of **6b**, which is highly stabilized in the polar solvent.

(14) The same experiment in acetonitrile provided only one emission maximum (452 nm) and the corresponding excitation maximum (350 nm) (Figure S10).

(15) (a) Beens, H.; Knibbe, H.; Weller, A. *J. Chem. Phys.* **1967**, *47*, 1183. (b) Lippert, E. *Z. Naturforsch.* **1955**, *10a*, 541. (c) Mataga, N.; Kaifu, Y.; Koizumi, M. *Bull. Chem. Soc. Jpn.* **1956**, *29*, 465.

(16) See the Supporting Information for the Lippert−Mataga plots of emissions A and B, estimation of the Onsager radii, and calculation of the differences of dipole moments $|\mu_e - \mu_g|$.

(17) For reviews of mechanofluorochromism, see: (a) Sagara, Y.; Kato, T. *Nat. Chem.* **2009**, *1*, 605. (b) Balch, A. L. *Angew. Chem., Int. Ed.* **2009**, *48*, 2641. (c) Chi, Z.; Zhang, X.; Xu, B.; Zhou, X.; Ma, C.; Zhang, Y.; Liu, S.; Xu, J. *Chem. Soc. Rev.* **2012**, *41*, 3878. (d) Sagara, Y.; Yamane, S.; Mitani, M.; Weder, C.; Kato, T. *Adv. Mater.* **2016**, *28*, 1073.

(18) See the Supporting Information for the emission profiles.

(19) The elongation of the emission lifetime by grinding of **6b** demonstrates that the red shift of the fluorescence is likely due to excimer formation (Figures S11 and S12).

DOI: 10.1021/acs.orglett.6b01786
Org. Lett. 2016, 18, 3988−3991